Electronic Supplementary Information for:

High Contrast Solid State Electrochromic Devices based on Ruthenium Purple Nanocomposites Fabricated by Layer-by-Layer Assembly

Vaibhav Jain, Rabindra Sahoo, Joerg R. Jinschek, Reza Montazami, Hank M. Yochum, Fredrick L. Beyer, Anil Kumar, James R. Heflin*

* Email: rheflin@vt.edu

Characterization of Ruthenium Purple (RuP) nanoparticles:

High resolution transmission electron microscope (HRTEM) images were obtained on a FEI Titan 300 at an accelerating voltage of 200kV. Samples for TEM analysis were prepared by spreading a drop of dilute dispersion of as-prepared products on thin (3nm) amorphous carbon-coated copper grids (Ted Pella Inc) and then dried in air. The average particle size and its standard deviation was estimated from HRTEM image analysis of 100 particles at 200 keV.

X-ray diffraction (XRD) patterns of the products were recorded using a Rigaku Ultrax 18 rotating anode X-Ray generator operating at 60 kV and 40 mA. A pyrolytic graphite monochromator was used to filter out all radiation except the CuKα doublet, with an average wavelength of λ = 1.5418 Å. No background corrections were applied. The powder form of the nanoparticles was obtained by drying the concentrated solution of RuP on a glass slide placed on a hot plate and then scraping the film. The DLS size and zeta potential measurements were performed with a Zetasizer nanoZS (Malvern Instruments) operating at a fixed angle of 173° and 633 nm wavelength. To remove the large nanoparticle agglomerates, the diluted ruthenium purple solution was passed through a 100 nm Teflon filter.

XPS spectra were obtained on a PHI Perkin-Elmer Model 5400 photoelectron spectrometer. The excitation radiation was a Mg Kα X-ray ($h\nu = 1253.6$ eV). The X-ray generator was operated at 14 kV and 300 watts. A PHI 10-360 hemispherical energy analyzer was used which operated in the constant pass energy (E_0) mode, where $E_0 = 44.75$ eV for survey scans and $E_0 = 17.9$ eV for high-resolution narrow scans. The vacuum was maintained below 5×10^{-7} torr during analysis. The XPS spectra were obtained at a take-off angle of 45° with respect to the surface of the sample unless otherwise noted. Initially a wide scan spectrum (survey scan) over a binding energy range of 1 to 1100 eV was obtained. All the elements were then identified from their binding energies, and then a narrow scan was carried out for each element identified in the survey scan. The atomic ratio of the atoms in the LbL film is calculated from their relative peak areas after correction of the sensitivity factors. XPS spectra of the 40 bilayer LPEI/RuP film show nearly 1:1 atomic concentration of Fe and Ru.

UV-vis spectra were recorded in a Perkin Elmer Lambda 25 UV-Vis spectrophotometer. Switching of the devices was monitored over time with a He-Ne laser (633 nm) and photodiode as the square wave voltage from -1.0V to +0.8 V was applied to the solid-state electrochromic device. The switching time for coloration and a de-coloration time is for 70% overall change in transmittance at switching voltages of -1.0V and +0.8 V.

All electrochemical experiments were carried out in a EG&G PAR model 362 potentiostat/galvanostat and a PINE AFCBP1 bipotentiostat controlled by Pine Chem. Software in a three electrode cell, with Ag/Ag+(0.01 M $AgNO_3$/ACN) as the reference electrode and a platinum flag as the counter electrode. The CV experiment was performed in 0.1M $LiClO_4$ /acetonitrile (ACN) electrolyte solution at 50mV/s scan rate.

Calculation of the Coloration Efficiency (η):

Coloration Efficiency defined at the wavelength maximum λ_{max} (560nm in our case)is the relationship between the changes in optical density to the total injected/ejected charge as a function of the electrode area. Change in the transmittance state from colorless to dark purple gives an optical density of

$$\Delta \text{ OD} = \log [T_b(\lambda)/ T_c(\lambda)]$$

$$= 0.853$$

$$\eta (\lambda) = \Delta \text{ OD}/Q_d$$

where $Q_d = 4.16$ mC/cm^2 for the reduction step and is calculated as the area under the CV curve for the reduction peak for the scan rate of 50 mV/s. The active working area of the film on the ITO electrode was 10 cm^2.

Hence, $\eta (\lambda) = 205$ cm^2/C

LbL Film Fabrication:

An automated dipping machine from Nanostrata Inc. was used for deposition of the multilayer films. For LbL assembly, ITO substrates were first washed with water to develop some negative charge and then alternately dipped in 10 mM solution of linear polyethylene imine (LPEI) at pH 4 and 5 mM solution of RuP at pH 4 for 6 mins each, followed by 3-step of rigorous -rinsing with deionized water for 45 secs after each deposition step. The linear increase in absorbance with increased number of bilayers (Figure S1) demonstrates that an equal amount of material is deposited with every bilayer. Linearity in the absorbance is observed as high as 160 bilayers, showing that thick films can be easily formed without disturbing the overall morphology or surface coverage per bilayer.

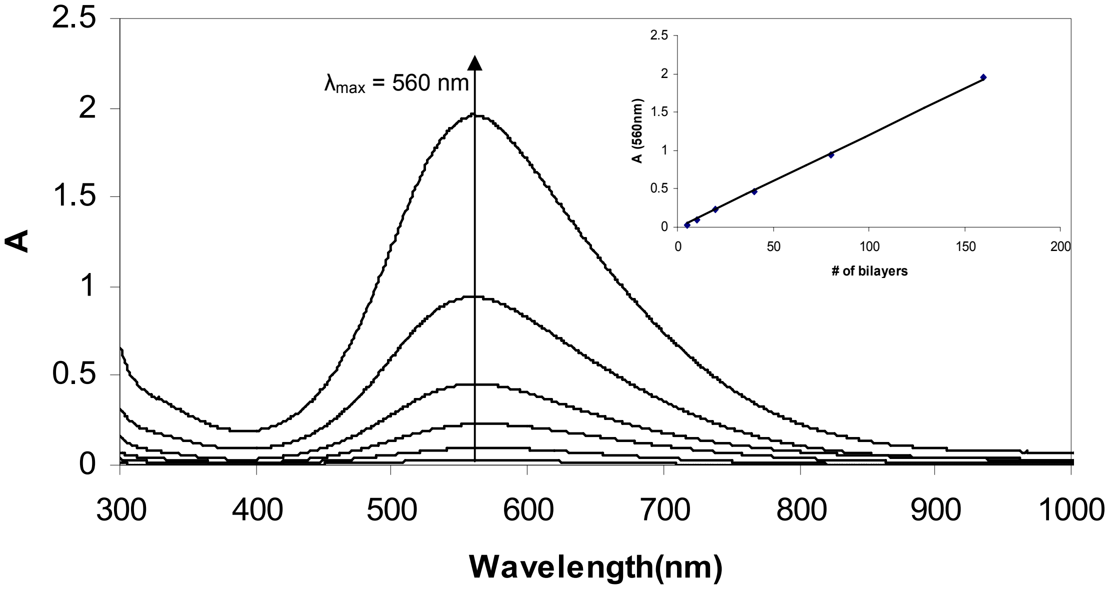

Figure S1. Absorbance versus number of bilayers of the LPEI/RuP nanocomposite film. Inset is the linear increase in the absorbance (at 560 nm) of LPEI/RuP film with number of bilayers.

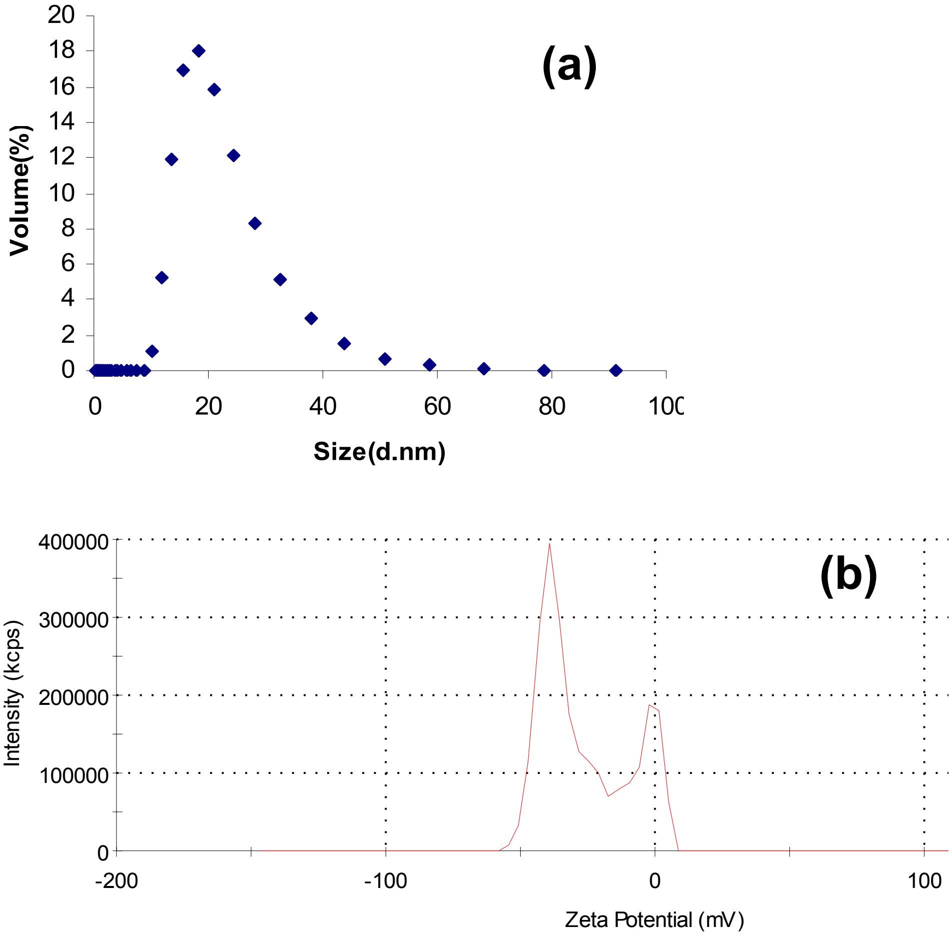

Figure S2. (a) Dynamic Light Scattering (DLS) and (b) zeta potential measurements of the aqueous dispersion of as-synthesized RuP nanoparticles.

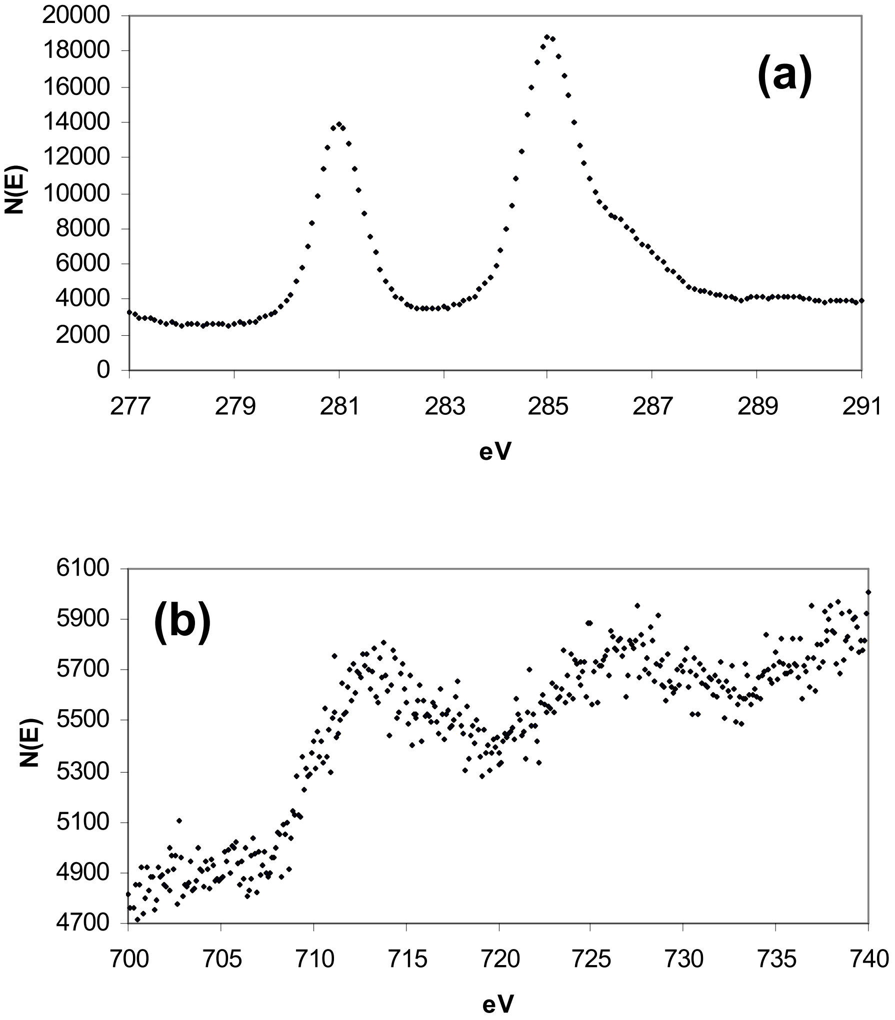

Figure S3. The a) Ru $3d^5$ and b) Fe 2p high resolution X-ray photoelectron spectra (XPS) of a 20 bilayer LBL film of LPEI/RuP.

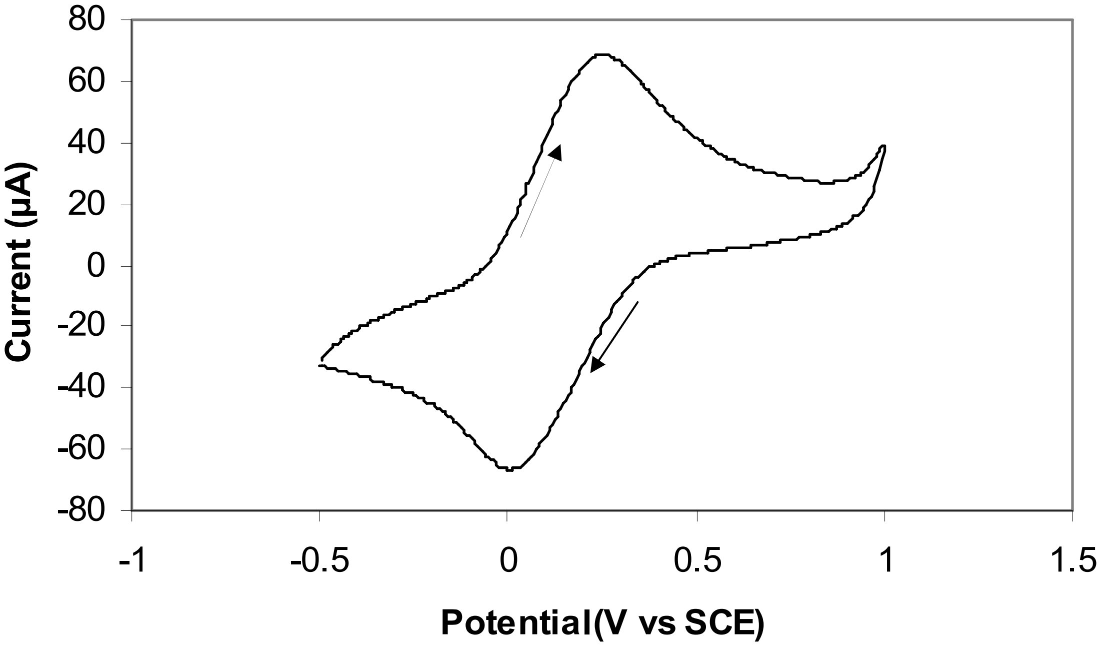

Figure S4. Cyclic voltammetry of a 40 bilayer LPEI/RuP film in 0.1M $LiClO_4$ /ACN electrolyte solution at 50 mV/s scan rate.

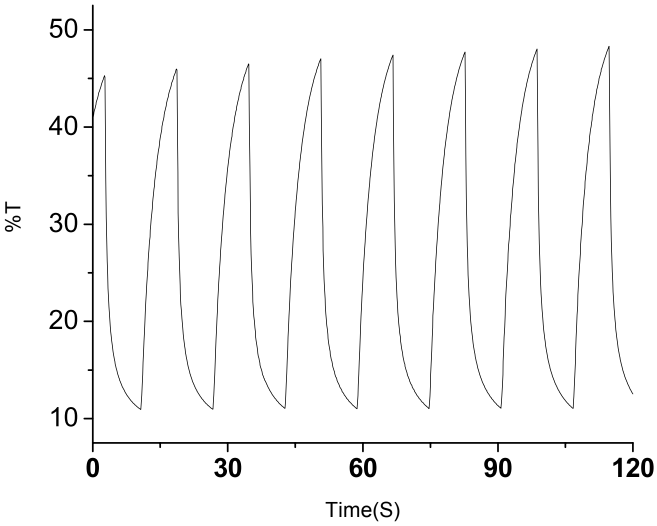

Figure S 5: Liquid electrolyte optical switching of a single 40 bilayer LPEI/RuP film immersed in 0.1M LiClO4/ACN with delay time of 8 sec.